K-isomeric states in the isotopic and isotonic chains of ^{178}Hf

N. Minkov [*]

Institute for Nuclear Research and Nuclear Energy, Bulgarian Academy of Sciences, Tzarigrad Road 72, BG-1784 Sofia, Bulgaria

L. Bonneau [†] and P. Quentin

LP2I Bordeaux, UMR 5797, Université de Bordeaux, CNRS, F-33170 Gradignan, France

J. Bartel and H. Molique

IPHC, UMR 7178, Université de Strasbourg, CNRS, F-67000 Strasbourg, France

Meng-Hock Koh (辜 明 福)

*Department of Physics, Faculty of Science, Universiti Teknologi Malaysia, 81310 Johor Bahru, Johor, Malaysia
and UTM Centre for Industrial and Applied Mathematics, 81310 Johor Bahru, Johor, Malaysia*

We study the evolution of $K^\pi = 6^+$ and 8^- two-quasiparticle (q.p.) configurations in the isotopic and isotonic chains of even-even deformed nuclei around ^{178}Hf and their ability to describe series of observed K-isomer excitations within the framework of a Skyrme Hartree-Fock-BCS (SHFBCS) approach using SIII interaction and seniority pairing strengths with self-consistent blocking. We apply the approach along the prescription of Minkov *et al.* [Phys. Rev. C **105**, 044329 (2022)] used to describe K isomers in the actinide and transfermium mass regions. The calculations allow us to identify the regions where proton or neutron configurations or their mixture may be responsible for the K-isomer formation. The obtained results provide a detailed test for the Skyrme SIII interaction used and outline the limits of applicability of the overall SHFBCS approach in the regions of well deformed nuclei. The study suggests that similar systematic analysis can be implemented in the heavier mass regions whenever enough data are available.

I. INTRODUCTION

More than a century after their discovery, nuclear isomers [1,2] remain one of the most exciting subjects in the nuclear structure study [3]. In particular, the K isomers, for which a continuous stream of data comes from the nowadays advanced experimental facilities, provide new detailed information about the intrinsic shell-structure configurations which govern the appearance of nuclear metastable states, offering at the same time a stringent test for the effective interactions used in the many-body theories of the nucleus. In the last decade the wealth of data has firmly expanded from the regions of moderate masses, such as the rare-earth and translanthanide ($72 \leqslant Z \leqslant 82$) nuclei [4] (for recent works see [5–7]), to the region of very heavy and superheavy nuclei [8–16] (for recent comprehensive review on transuranium nuclei see [17]). Up to date collections of data on nuclear isomers are available in [18] and [19].

These experimental developments have been mirrored by a number of model descriptions within diverse theoretical approaches ranging from Nilsson-Strutinsky or Woods-Saxon mean fields [20] (see references therein) to many-body self-consistent theories [21]. In the former direction an advance in the K-isomer study was made through the so-called configuration-constrained energy surfaces in which the Nilsson quantum numbers of given single-particle (s.p.) configuration responsible for the isomer formation are traced through level crossings over the deformation surface (e.g., see [22–24] for applications to transactinides and superheavy nuclei). Further development in this direction was made by using the configuration-constrained rotation approach [25,26] and the projected shell model (e.g., see [27–29] for applications in rare-earth and heavier nuclei) allowing for the study of rotation spectra built on K-isomeric states. More recent progress in the K-isomer study was made in the framework of the cranked Nilsson shell model with high-multipolarity deformations and particle-number conservation achieved through diagonalization of the Hamiltonian in an appropriately truncated cranked many-particle configuration space (see [30–32] for applications to neutron-rich rare-earth nuclei and ^{254}No). Regarding the Woods-Saxon potential, it was applied in a deformed shell model with pairing interaction to study the influence of octupole deformation on the two-q.p. energy and magnetic moments in the K-isomeric states in the range from rare-earth to actinide and transfermium nuclei including ^{270}Ds [33]. An advanced use of the Woods-Saxon mean field

---

[*]Contact author: nminkov@inrne.bas.bg

[†]Contact author: bonneau@lp2ib.in2p3.fr

was made in a macroscopic-microscopic model framework allowing for the prediction of a large amount of multi-q.p. configurations candidates for high-K isomeric states in very heavy and superheavy nuclei [34–36]. A macroscopic-microscopic approach based on a two-center shell model has been also applied for the prediction of variety of K-isomeric states in superheavy nuclei [37] as well as for the study of the Coriolis mixing effect on the isomer lifetimes in heavy nuclei [38].

In the latter direction—many-body self-consistent theories—it has been shown that the energy-density-functional (EDF) theory, in its nonrelativistic Skyrme and Gogny as well as relativistic (covariant density functional) realizations, is capable of reproducing q.p. spectra in heavy nuclei [39] (see references therein). A deformed Hartree-Fock (HF) approach with surface delta residual interaction and angular momentum projection was applied to describe known K-isomers—and predict possible unobserved ones—in the rare-earth mass region (Gd and Dy isotopes) [40]. In a recent work of the present authors a Skyrme Hartree-Fock-BCS (SHFBCS) approach with SIII interaction and self-consistent blocking was applied to describe two-q.p. energies and predict magnetic dipole moments in K-isomeric states of actinide and transfermium nuclei [41]. Also in a recent work, a Hartree-Fock-Bogoliubov (HFB) approach with density-dependent Gogny force used with both blocking and equal filling approximations was successfully applied to two- and four-q.p. K-isomeric states in ^{254}No, ^{178}Hf and several nuclei of the tungsten isotopic chain [42]. An advanced application of the covariant density functional theory (CDFT) was made in works [43,44], where relativistic Hartree-Bogoliubov (RHB) calculations with blocking and time-reversal symmetry breaking were performed for two-q.p. K-isomer configurations in transactinide nuclei around $N = 162$ [43] and nuclei in the region from Er to Pb [44].

We remark that while in the transactinide and superheavy nuclei the collection of data on K-isomers still needs to expand, in the rare-earth and translanthanide nuclei the available data already encompass rather long continuous chains of isotopes and isotones [4]. The latter allow one not only to follow the evolution of the particular proton or neutron configurations in the K-isomer structure, but also to examine the capability of the effective interactions to reproduce it as well as to explore the limits of applicability of the model approximations used. Such a study was made in the above mentioned Ref. [44] (in the CDFT framework), where the RHB calculations performed for the $K^\pi = 6^+$ and 8^- isomeric energies in the hafnium isotopic and $N = 104, 106$ isotonic chains provided a detailed test of the used density-dependent meson-exchange DD-ME2 and point-coupling DD-PC1 functionals. On the other hand, so far similar investigations within the non-relativistic EDF approach, especially using Skyrme effective interaction, have not been done in this mass region. Moreover, except for the recent SHFBCS study in the transactinide region [41], to our knowledge no other specific application of the Skyrme EDF was made to investigate K-isomeric states. A number of works such as Ref. [39] (and works quoted therein) describe a variety of q.p. excitations

in nuclei of different mass regions, but without particular focus on K-isomer properties (see also [45–47]). In this aspect testing the Skyrme effective interaction on the long isotopic and isotonic series of K-isomeric states in the rare-earth nuclei would be important not only for assessing the force itself but also for achieving a new specific explanation of the observed and predicted systematic behavior of the s.p. excitations and nuclear shell structure in this mass region.

Motivated by the above, the purpose of the present work is to explore the series of K-isomeric states in the isotopic and isotonic chains to which ^{178}Hf belongs with the use of the Skyrme EDF. Based on the success of our recent work on transactinide nuclei [41] we now assess for the first time the capability of the Skyrme effective interaction to reproduce the systematic behavior of K-isomer energies and magnetic dipole moments in the long series of nuclei in the rare-earth and translanthanide region. We thoroughly examine the relevance of different proton and neutron two-q.p. configurations and their potential mixing to explain the formation mechanism and properties of the K-isomer excitations in dependence on the underlying nuclear shell structure.

We consider the series of $K^\pi = 6^+$ and 8^- two-quasiparticle (q.p.) excitations in the isotopic chains of $^{168-184}$Hf and $^{170-186}$Hf, respectively, and the $K^\pi = 8^-$ series in the $N = 106$ isotonic chain from ^{170}Gd to ^{182}Os. As usual K and π denote respectively the projection of the total nuclear angular momentum on the symmetry axis in the body-fixed frame and the intrinsic parity. We apply a selfconsistent Skyrme-Hartree-Fock plus Bardeen-Cooper-Schrieffer (SHFBCS) approach with the SIII parametrization [48] to calculate the $K^\pi = 6^+$ and 8^- excitation energies using the same numerical algorithm as for the description of K isomers in the regions of heavy actinide and transfermium nuclei [41]. The configurations to be blocked are determined as follows:

(i) For the $K^\pi = 6^+$ isomeric state we consider the two-neutron $(\frac{5}{2}^-[512], \frac{7}{2}^-[514])_n$ and the two-proton $(\frac{5}{2}^+[402], \frac{7}{2}^+[404])_p$ blocked configurations, which are the lowest two in the ^{178}Hf nucleus, and follow them in even-A Hf isotopes between $A = 168$ and $A = 186$.

(ii) For the $K^\pi = 8^-$ states, we take the two-neutron $(\frac{7}{2}^-[514], \frac{9}{2}^+[624])_n$ and the two-proton $(\frac{7}{2}^+[404], \frac{9}{2}^-[514])_p$ blocked configurations, which are the lowest two in the ^{178}Hf nucleus, and follow them in Hf isotopes between $A = 168$ and $A = 186$, and in $N = 106$ even-A isotones between $A = 170$ and $A = 182$.

When relevant, we also consider energetically favorable alternate configurations (see Sec. III).

As will be shown below, the obtained series of theoretical energy levels and attendant magnetic moments compared to experimental data allow us to identify the configurations most probably contributing to the formation of the considered K-isomer excitations along the corresponding chains of nuclei. Also, the comparison with other theoretical approaches, such as the CDFT applied in the same mass region [44], allows us to

assess on the same footing the applicability of the SIII Skyrme parametrization in the study of nuclear *K*-isomer excitations.

In Sec. II we briefly present the SHFBCS approach used together with some details on the pairing and basis parameters choice and the computational algorithm. Numerical results are presented and discussed in Sec. III, before presenting some concluding remarks in Sec. IV.

II. THEORETICAL FRAMEWORK

The theoretical approach used here includes a Skyrme HFBCS energy-density functional with cylindrical symmetry (axial deformation) in the intrinsic frame and self-consistent blocking of the single-particle orbitals entering the excited two-quasiparticle configuration [41]. We employ the SIII Skyrme parametrization [48] within a "minimal" scheme including the spin and current vector time-odd fields only, as explained in Ref. [49]. The latter cause a time-reversal symmetry breaking at the one-body level in the excited states leading via the self-consistent blocking to a removal of the Kramers degeneracy in the single-particle energy spectrum.

The HF Hamiltonian is diagonalized and the single-particle spectrum is obtained as an expansion in the axially deformed harmonic-oscillator basis [50] truncated at the $N_0 + 1 = 15$ major oscillator shell. The matrix elements are calculated through quadratures using 30 Gauss-Hermite mesh points in the *z* direction and 15 Gauss-Laguerre mesh points in the perpendicular direction. The basis parameters *b* and *q* (defined in Ref. [50]) are optimized for the considered nuclei. Because the resulting parameters vary only marginally over the considered chains of isotopes and isotones, with a very small effect on excitation energies of less than a couple of tens of keV (barely visible in the figures below) and on magnetic moments of a few thousands of the nuclear magneton μ_N, we retain the same values $b = 0.480$ and $q = 1.185$ for all nuclei. Moreover this allows us to make comparisons between different nuclei with the same single-particle basis.

The pairing correlations are taken into account through the expectation values of a seniority residual interaction in the BCS states with a subsequent blocking at each iteration of the single-particle states entering the excited state configuration. The nucleon-number dependence of the corresponding matrix elements is parameterized as in Ref. [49]. The BCS equations are solved for all single-particle states with a smearing factor $f(e_i) = [1 + \exp((e_i - X - \lambda_\tau)/\mu)]^{-1}$ where e_i is the energy of the single-particle state $|i\rangle$, $X = 6$ MeV is a truncation parameter, λ_τ is the chemical potential for $\tau = n, p$ (neutrons and protons), and $\mu = 0.2$ MeV is a diffuseness parameter. The neutron and proton pairing-strength constants are taken for all considered nuclei as $G_n = 16$ MeV and $G_p = 15$ MeV based on earlier proposed concept of overall adjustment with respect to experimental estimations for the moment of inertia [51] (see also Sec. IV in Ref. [41]).

The theoretical two-quasiparticle excitation energy is determined as

$$E^*_{th}(K^\pi) = E^{2qp}_{tot}(K^\pi) - E^{GS}_{tot}, \qquad (1)$$

where $E^{2qp}_{tot}(K^\pi)$ is the total HFBCS energy of the nucleus, obtained in the solution with blocked isomer configuration

orbitals and E^{GS}_{tot} is the total energy in the ground-state solution. We emphasize that here the *K*-isomer excitation energy is not simply the sum of the quasiparticle energies of two neutrons/protons that would be calculated from the GS solution. As a difference between the total energies obtained in the solutions for the blocked 2q.p. configuration and the ground state, $E^*_{th}(K^\pi)$ incorporates the relevant nuclear bulk properties determined in the self-consistent calculations. Also, we note that although the HFBCS is not a configuration-mixing approach it takes into account the quasiparticle interaction through the one-body reduction of the two-nucleon potential. The same is valid for the CDFT approach used in [43,44]. As mentioned in Sec. I the relevance of the Skyrme EDF for the description of q.p. excited bandheads was pointed out in a number of earlier works (e.g., see Refs. [39,45–47]), while the particular use of the Skyrme SIII parametrization for description of *K*-isomer excitations in transactinide nuclei was demonstrated in our recent work [41]. Moreover, the latter was proved to be capable of describing *K*-isomeric states in the presence of octupole deformation [52].

The magnetic dipole moments in the two-quasiparticle configurations are calculated by taking into account core-polarization effects as explained in Ref. [49]. In the same reference, the particular choice made to estimate the collective gyromagnetic ratio [as calculated in Eq. (13) of Ref. [49]] is detailed: (i) the BCS pairs are built from s.p. canonical basis states which are almost time conjugated, (ii) the blocked pairs are removed from the summations, and (iii) the same quasiparticle energy is used for both members of a BCS pair.

III. NUMERICAL RESULTS AND DISCUSSION

We performed numerical SHFBCS calculations for the $K^\pi = 6^+$ and 8^- lowest-energy neutron and proton two-quasiparticle configurations in the isotopic and isotonic chains of well-deformed nuclei around ^{178}Hf, as explained above. The results are given in Tables I and II, where the deformation characteristics of the considered isotopes/isotones are expressed by the experimental $R_{42} = E(4^+_1)/E(2^+_1)$ ratio of the energies of the first two members of the ground-state rotational band. For a good rotator the R_{42} value should be larger than or of the order of 3.2. For each nucleus we compare the obtained neutron and proton two-quasiparticle excitation energy $E^{*\tau}_{th}(K^\pi)$ ($\tau = n, p$) with the experimental value for the corresponding *K*-isomeric state [4,18]. In a few cases, where no data are available, we still give the theoretical predictions for better understanding of the evolution of isomeric energies along the considered isotopic and isotonic chains. In the tables we also give theoretical magnetic dipole moments calculated for each two-quasiparticle configuration and compare them with experimental data where available.

It should be noted that the considered Hf isotopes are part of the region of collective rotation with an experimental R_{42} ratio varying in the range 3.11–3.19 in $^{168-170}$Hf and a value of 3.31 in ^{180}Hf [53] (see Table I). The corresponding quadrupole deformation parameter β takes values $\beta \approx$ 0.27–0.28 in ^{168}Hf and ^{180}Hf and $\beta \approx$ 0.30–0.31 in $^{170-176}$Hf [54]. In the considered $N = 106$ even isotones, the good-rotor character is experimentally confirmed only from ^{176}Yb to

TABLE I. Theoretical (HFBCS) excitation energies E_{th}^{*n} and E_{th}^{*p} (in MeV) and magnetic dipole moments μ_{th}^n and μ_{th}^p (in nuclear magneton units) for the lowest-energy neutron and lowest-energy proton $K^\pi = 6^+$ and $K^\pi = 8^-$ configurations in even Hf ($Z = 72$) isotopes from $A = 168$ to $A = 186$, compared with the experimental $K^\pi = 6^+$ [4] and $K^\pi = 8^-$ [18] isomeric energies (except for the 8^- isomeric energy in ^{170}Hf taken from Ref. [19]) Magnetic dipole moments are taken from Refs. [56,57] (with the published references). Experimental R_{42} ratios [53] are also given (third column). Blank entries correspond to missing data.

A	N	R_{42}	K^π	Neutron configuration	E_{th}^{*n}	Proton configuration	E_{th}^{*p}	E_{exp}^*	μ_{th}^n	μ_{th}^p	μ_{exp}
168	96	3.110	6^+	$(5/2^+[642], 7/2^+[633])$	2.626	$(5/2^+[402], 7/2^+[404])$	2.236		-1.249	5.740	
			8^-	$(7/2^-[514], 9/2^+[624])$	5.277	$(7/2^+[404], 9/2^-[514])$	2.348		0.251	7.399	
170	98	3.194	6^+	$(5/2^+[642], 7/2^+[633])$	1.821	$(5/2^+[402], 7/2^+[404])$	2.301	1.773	-1.357	5.652	
			8^-	$(7/2^-[514], 9/2^+[624])$	4.663	$(7/2^+[404], 9/2^-[514])$	2.265	2.183	0.148	7.348	
172	100	3.248	6^+	$(5/2^+[642], 7/2^+[633])$	2.283	$(5/2^+[402], 7/2^+[404])$	2.339	1.685	-1.284	5.670	$+5.6(6)$[58]
			8^-	$(7/2^-[514], 9/2^+[624])$	3.722	$(7/2^+[404], 9/2^-[514])$	2.129	2.006	0.062	7.338	$+7.93(6)$[58]
174	102	3.268	6^+	$(5/2^-[512], 7/2^-[514])$	2.069	$(5/2^+[402], 7/2^+[404])$	2.279	1.549	0.073	5.676	$+5.40(5)$[58]
			8^-	$(7/2^-[514], 9/2^+[624])$	2.774	$(7/2^+[404], 9/2^-[514])$	1.910	1.798	0.150	7.335	
176	104	3.284	6^+	$(5/2^-[512], 7/2^-[514])$	1.061	$(5/2^+[402], 7/2^+[404])$	2.159	1.333	-0.029	5.697	
			8^-	$(7/2^-[514], 9/2^+[624])$	1.737	$(7/2^+[404], 9/2^-[514])$	1.598	1.559	0.267	7.342	7.93
178	106	3.291	6^+	$(5/2^-[512], 7/2^-[514])$	1.913	$(5/2^+[402], 7/2^+[404])$	2.143	1.554	0.106	5.703	$+5.81(5)$[58]
			8^-	$(7/2^-[514], 9/2^+[624])$	1.136	$(7/2^+[404], 9/2^-[514])$	1.349	1.147	0.312	7.349	$+3.09(1)$[59]
180	108	3.307	6^+	$(5/2^-[512], 7/2^-[514])$	3.748	$(5/2^+[402], 7/2^+[404])$	2.194	1.703	0.168	5.695	
			8^-	$(7/2^-[503], 9/2^+[624])$	3.009	$(7/2^+[404], 9/2^-[514])$	1.179	1.142	-1.922	7.342	$+8.7(10)$[60]
182	110	3.295	6^+	$(5/2^-[512], 7/2^-[503])$	4.010	$(5/2^+[402], 7/2^+[404])$	2.223		-2.050	5.755	
			8^-	$(7/2^-[503], 9/2^+[624])$	3.204	$(7/2^+[404], 9/2^-[514])$	1.081	1.173	-1.879	7.378	
184	112	3.264	6^+	$(5/2^-[512], 7/2^-[503])$	4.052	$(5/2^+[402], 7/2^+[404])$	2.264		-2.042	5.822	
			8^-	$(7/2^-[503], 9/2^+[624])$	3.228	$(7/2^+[404], 9/2^-[514])$	1.024	1.272	-1.929	7.414	
186	114		6^+	$(5/2^-[512], 7/2^-[503])$	4.091	$(5/2^+[402], 7/2^+[404])$	2.290		-2.021	5.895	
			8^-	$(7/2^-[503], 9/2^+[624])$	3.209	$(7/2^+[404], 9/2^-[514])$	1.057		-2.032	7.455	

^{180}W ($R_{42} \approx 3.3$), whereas the R_{42} value is somewhat lower in ^{182}Os (about 3.15) and experimental data for ^{170}Gd up to ^{174}Er are unavailable in Ref. [53].

A. Isomeric energies

The energy levels obtained in our calculations for $K^\pi = 6^+$ excitations in the $^{168-186}$Hf isotopic chain are plotted in Fig. 1 as function of the neutron number. One finds that the en-

TABLE II. Theoretical (HFBCS) excitation energies E_{th}^{*n} and E_{th}^{*p} (in MeV) and magnetic dipole moments μ_{th}^n and μ_{th}^p (in nuclear magneton units) for the lowest-energy $K^\pi = 8^-$ neutron $(\frac{7}{2}^-[514], \frac{9}{2}^+[624])$ and proton $(\frac{7}{2}^+[404], \frac{9}{2}^-[514])$ configurations, in even $N = 106$ isotones from $A = 170$ to $A = 182$, compared with the experimental $K^\pi = 8^-$ isomeric energies [4] and magnetic dipole moments given by Refs. [56,57] (with the published references). Experimental R_{42} ratios [53] are also given. Blank entries correspond to missing data.

Nucleus	R_{42}	E_{th}^{*n}	E_{th}^{*p}	E_{exp}^*	μ_{th}^n	μ_{th}^p	μ_{exp}
$^{170}_{64}$Gd		1.118	6.746		0.331	7.491	
$^{172}_{66}$Dy		1.060	5.629	1.278	0.356	7.520	
$^{174}_{68}$Er		1.018	4.328	1.112	0.334	7.571	
$^{176}_{70}$Yb	3.31	1.028	3.012	1.050	0.334	7.422	$-0.151(15)$[59]
$^{178}_{72}$Hf	3.291	1.136	1.349	1.147	0.312	7.349	$+3.09(1)$[59]
$^{180}_{74}$W	3.26	1.276	2.465	1.529	0.256	7.354	
$^{182}_{76}$Os	3.154	1.365	3.314	1.831	0.253	7.391	

ergies corresponding to the two-proton $(\frac{5}{2}^+[402], \frac{7}{2}^+[404])_p$ blocked configuration (red bars) follow the overall behavior of experimental data, overestimating them by between 0.5 and 0.8 MeV (see also Table I). On the other hand the energy levels
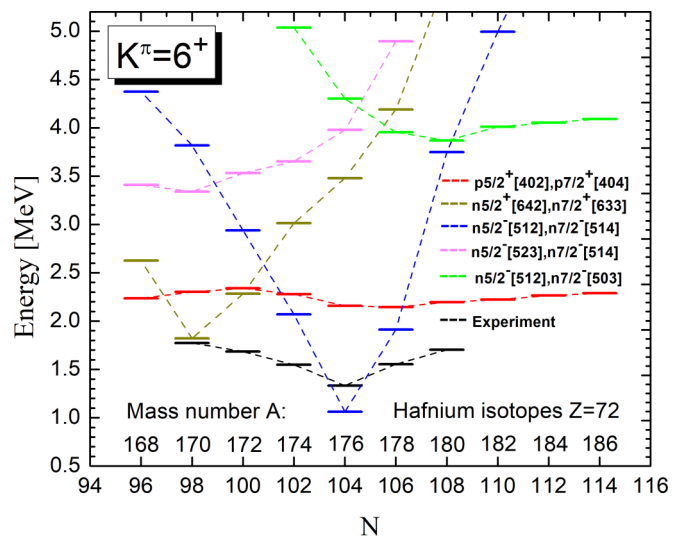
FIG. 1. Theoretical $K^\pi = 6^+$ excitation energies of low-lying two-neutron and two-proton blocked configurations obtained in even Hf isotopes from $A = 168$ to $A = 186$ compared with experimental data (in black) [4].

obtained with the two-neutron ($\frac{5}{2}^-$[512], $\frac{7}{2}^-$[514]) blocked configuration (blue bars) approach the experimental levels more closely in $^{174-178}$Hf isotopes, but yield much too high excitation energies for lighter and heavier Hf isotopes. In ^{176}Hf the theoretical value of $E_{\text{th}}^{*n}(6^+) = 1.061$ MeV underestimates the experimental value of 1.333 MeV by 272 keV while in ^{174}Hf and ^{178}Hf the calculations overestimate the experimental value by 520 and 359 keV, respectively (see Table I). One may thus consider that in ^{176}Hf the structure of the 6^+ isomer is dominated by the two-neutron ($\frac{5}{2}^-$[512], $\frac{7}{2}^-$[514]) configuration while for ^{174}Hf and ^{178}Hf some admixture with the two-proton ($\frac{5}{2}^+$[402], $\frac{7}{2}^+$[404]) configuration is likely to occur. The latter was actually found experimentally a long time ago from two-nucleon transfer reactions in ^{178}Hf with a dominance (69%) of the ($\frac{5}{2}^+$, $\frac{7}{2}^+$) proton configuration with the Nilsson quantum numbers [402] and [404] (see Table I of Ref. [55]). Further away from these three Hf isotopes, the two-neutron ($\frac{5}{2}^-$[512], $\frac{7}{2}^-$[514]) configuration is definitely off, while the two-proton configuration still follows the experiment from above.

One notices that in the above considered $K^\pi = 6^+$ excitations the leading components of the calculated single-particle wave functions in the axially deformed harmonic-oscillator expansion, namely ($\frac{5}{2}^-$[512], $\frac{7}{2}^-$[514]) for the two-neutron configuration and ($\frac{5}{2}^+$[402], $\frac{7}{2}^+$[404]) for the two-proton configuration, agree with the Nilsson quantum numbers proposed earlier in the literature (see, e.g., [53] for references). However, we find an alternative configuration to account for the $K^\pi = 6^+$ isomer in the ^{170,172}Hf isotopes, namely the neutron ($\frac{5}{2}^+$[642], $\frac{7}{2}^+$[633]) two-quasiparticle configuration, as can be seen in Fig. 2 in the single-particle spectra of ^{170}Hf. In particular, a remarkable agreement with experiment is obtained for this configuration in ^{170}Hf.

Here it is interesting to make a comparison with the analogous result obtained in Ref. [44] through RHB calculations with DD-ME2 and DD-PC1 functionals. First, comparing our Fig. 1 with Fig. 6 in [44] (RHB with DD-ME2) we notice a similarity in the shapes of the energy curves for the two-neutron ($\frac{5}{2}^+$[642], $\frac{7}{2}^+$[633]), ($\frac{5}{2}^-$[512], $\frac{7}{2}^-$[514]) and two-proton ($\frac{5}{2}^+$[402], $\frac{7}{2}^+$[404]) configurations as functions of the neutron number N. However, in the RHB calculation the "neutron" curves show much shallower minimum with N while the "proton" curve appears higher in energy compared to our SHFBCS calculation. Then, comparing the energies of the lowest configurations obtained for the different isotopes in each calculation, our Table I and Table II in [44] (also compare our Fig. 1 with Fig. 7 in [44]), we see that for ^{170}Hf and ^{176}Hf the 6^+ energies obtained in the two approaches are rather similar. For ^{172}Hf and ^{174}Hf the RHB calculations provide better agreement with the experiment while for ^{178}Hf and ^{180}Hf better agreement is obtained in our SHFBCS calculation. The overall quality of the two model descriptions of the $K^\pi = 6^+$ excitations in Hafnium isotopes looks similar, which points to the similar spectroscopic characteristics of the interactions used in the two approaches. Further detailed comparison of the Skyrme SIII HFBCS approach and the RHB approach with DD-ME2 and DD-PC1 on the basis of K-isomer description might be valuable but is beyond the scope of this work.

Next, we investigate the $K^\pi = 8^-$ state with the two-neutron ($\frac{7}{2}^-$[514], $\frac{9}{2}^+$[624]) and two-proton ($\frac{7}{2}^+$[404], $\frac{9}{2}^-$[514]) blocked configurations. The obtained energy levels are plotted in Fig. 3 as functions of N. Similarly to the 6^+ isomer, we observe that the energy of the two-proton configuration closely follows the experimental energies, with an especially good agreement in ^{176}Hf and ^{180}Hf, with an overestimation of the experimental isomeric energies of only about 40 keV, as can be seen in Table I. At the same time the two-neutron configuration compares favorably with experiment only in the ^{176}Hf and ^{178}Hf isotopes, with an overestimation of about 180 keV in ^{176}Hf and an underestimation of only about 10 keV in ^{178}Hf. In the other isotopes the theoretical two-neutron blocked configuration energy is obtained high above the experimental energy and anyway at excitation energies where a description of excited states as being of a pure two-q.p. nature is most doubtful. Moreover one may note that for $A \geqslant 180$ the two-neutron ($\frac{7}{2}^-$[503], $\frac{9}{2}^+$[624]) configuration turns out to be energetically more favorable than the ($\frac{7}{2}^-$[514], $\frac{9}{2}^+$[624]) configuration.

For $N = 106$ the Fermi level lies in between the two $\frac{7}{2}^-$ and $\frac{9}{2}^+$ neutron s.p. levels relevant to form an 8^- two-q.p. configuration. The corresponding excitation energy lies slightly below the proton ($\frac{7}{2}^+$, $\frac{9}{2}^-$) configuration describing adequately the experimental 8^- isomeric states below $N = 104$ and above $N = 106$. As already pointed out long ago (see [55] and references quoted therein) the neutron-proton residual interaction yields a mixing of these two 8^- states in ^{178}Hf resulting in two states, the isomeric one at 1147 keV and another 338 keV above. As pointed out in Ref. [55] (see their Table I) the isomeric 8^- state is considered from two nucleons transfer data to be mostly of a neutron nature (64%). The fact that our neutron unperturbed state energy is lower than its proton counterpart points rightly in this direction.

Moving away from $N = 106$, apart from $N = 104$, the location of the Fermi level in the neutron s.p. spectra raises considerably the excitation energy of this two-q.p. neutron 8^- configuration, disqualifying it to describe the 8^- isomer. In ^{176}Hf the quasidegeneracy of the neutron $\frac{7}{2}^+$ and $\frac{1}{2}^-$ s.p. levels does not lower much the Fermi level below its $N = 106$ position, allowing for a mixing of the two neutron and proton configurations in the 8^- isomeric state where its proton component should probably be dominant in view of its lower unperturbed energy as compared to the neutron one.

The best reproduction of the 8^- isomeric energy is thus achieved in ^{176,178,180}Hf, which also represent the best rotators in the isotopic chain with $R_{42} = 3.28$–3.31 (see Table I). For all above considered $K^\pi = 8^-$ excitations the two-neutron configuration was obtained with the two-neutron ($\frac{7}{2}^-$[514], $\frac{9}{2}^+$[624]) configuration, while for the two-proton configuration we have ($\frac{7}{2}^+$[404], $\frac{9}{2}^-$[514]), again corroborating earlier proposed Nilsson quantum numbers in the structure of these configurations (see [53] and references therein). The above results outline an overall region of the most rele-
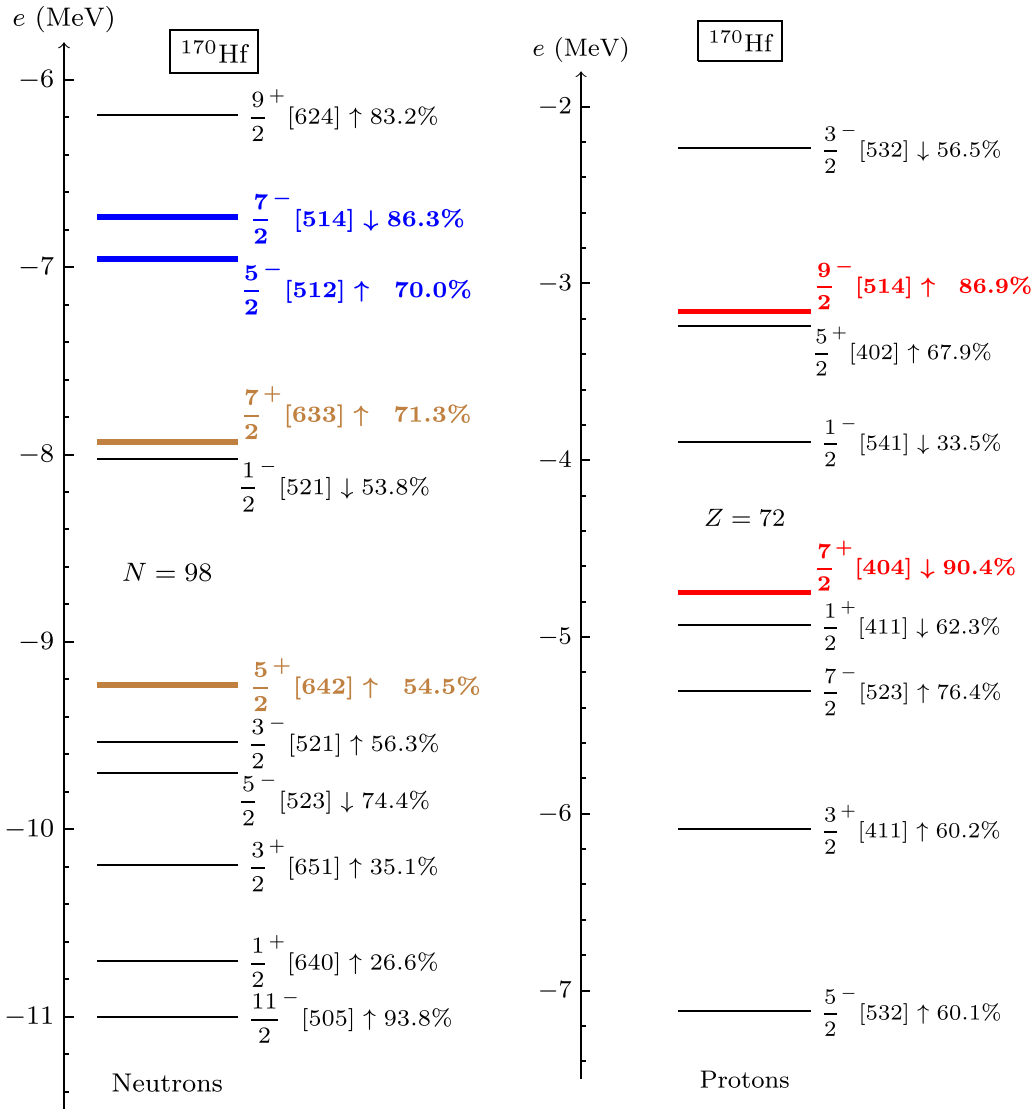
FIG. 2. Neutron and proton single-particle spectra in the ground-state solution of ^{170}Hf. Upward and downward arrows denote spin projections on the symmetry axis equal to $+1/2$ and $-1/2$, respectively, and the percentages given to their right are the weights of the corresponding Nilsson quantum numbers in the single-particle wave function. The boldface neutron levels in blue correspond to the lowest-energy ($\frac{5}{2}^-$[512], $\frac{7}{2}^-$[514]) neutron configuration of the $K^\pi = 6^+$ state in ^{178}Hf and neighboring even Hf isotopes, whereas the brown levels correspond to the lowest-energy neutron configuration in the ^{170,172}Hf isotopes. The boldface red proton levels identify the lowest-energy $K^\pi = 8^-$ proton configuration along the considered chain of even Hf isotopes.

vant applicability in the Hf isotopic chain of the SHFBCS approximation with SIII interaction. Here comparing again with Ref. [44] we notice a rather clear similarity in the shapes of the curves obtained for the energy of the two-proton configuration ($\frac{7}{2}^+$[404], $\frac{9}{2}^-$[514]) as a function of N in our calculation (Fig. 3) and in the RHB calculations with DD-ME2 and DD-PC1 functionals (Fig. 11 in [44]). Also, we notice the overall similarity in the quality of the two model descriptions (compare our Table I and Table IV in [44]).

In Fig. 4 the excitation energies corresponding to the $K^\pi = 8^-$ isomer in the $N = 106$ isotones are given as function of the proton number Z. One notices that the theoretical $E_{\text{th}}^{*n}(8^-)$ energy of the two-neutron ($\frac{7}{2}^-$, $\frac{9}{2}^+$)$_n$ configuration

is closer to the experimental isomer energies as compared to the two-proton configuration ($\frac{7}{2}^+$, $\frac{9}{2}^-$)$_p$ which approaches the experiment only in ^{178}Hf (overestimating it by 202 keV), while jumping to irrelevantly high values otherwise (see Table II and discussion above). The two-neutron configuration, on the contrary, provides a rather good agreement with the data for ^{176}Yb and for the above mentioned case of ^{178}Hf with an underestimation of respectively 22 and 11 keV. Aside from these two nuclei the disagreement between theory and experiment varies between a 90 and 470 keV underestimation along the isotonic chain from ^{172}Dy to ^{182}Os (see Table II). We remark that from ^{176}Yb to ^{182}Os the R_{42} ratio takes values between 3.31 and 3.15, which indicates their presence
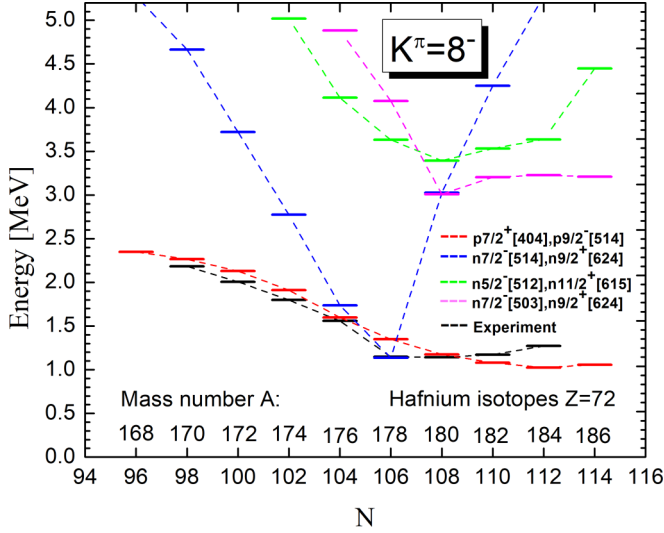
FIG. 3. Theoretical $K^\pi = 8^-$ excitation energies of low-lying two-neutron and two-proton blocked configurations obtained in even Hf isotopes from $A = 168$ to $A = 186$ compared with experimental data (in black) [18].

in the rotation part of the rare-earth region. No experimental information on R_{42} is available in [53] for ^{170}Gd, ^{172}Dy, and ^{174}Er, but one may guess that it should be close to the rotation values. In all considered $N = 106$ isotones we obtain the same Nilsson quantum numbers structure of the $K^\pi = 8^-$ two-neutron and two-proton configurations as in the case of the Hf isotopic chain discussed above. We may thus conclude that the present calculations provide reasonably motivated model predictions for the $K^\pi = 8^-$ isomer from ^{170}Gd to ^{180}W, which identifies the corresponding region of applicability of the present SHFBCS approach with the SIII parametrization.
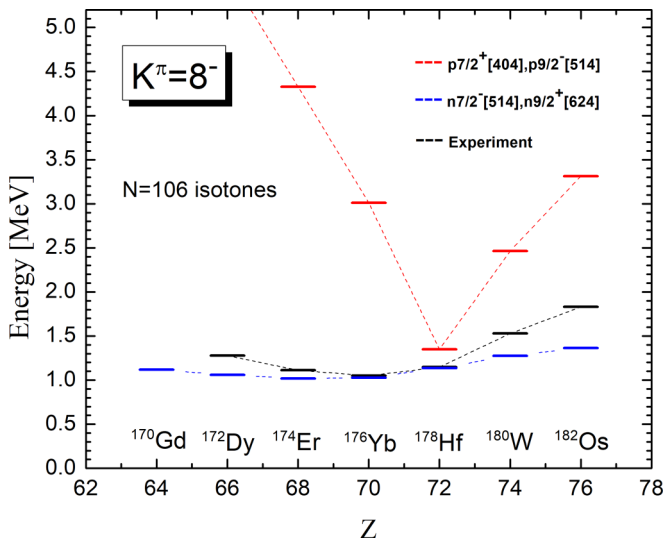
FIG. 4. Theoretical $K^\pi = 8^-$ two-quasiparticle excitation energies obtained from neutron (blue bars) and proton (red bars) two-quasiparticle configurations for the $N = 106$ isotonic chain between ^{170}Gd and ^{182}Os compared with experimental data (in black) [18].

Here the comparison with the RHB calculations of Ref. [44] shows the better quality of the present SIII HFBCS description (compare our Table II and Table V in Ref. [44]). Finding the source of discrepancy between the two approaches in the case would be an interesting subject of a separate study.

B. Magnetic dipole moment

Regarding the magnetic dipole moments, given in Tables I and II for the lowest-energy neutron and proton $K^\pi = 6^+$ and $K^\pi = 8^-$ configurations, we observe a rather stable behavior of the values calculated for the two-proton configurations. Indeed, along the $Z = 72$ isotopic chain, μ_{th}^p ranges for the $K^\pi = 6^+$ states roughly from $5.7 \, \mu_N$ to $5.9 \, \mu_N$, and for the $K^\pi = 8^-$ states roughly from $7.3 \, \mu_N$ to $7.4 \, \mu_N$. Similarly, along the $N = 106$ isotonic chain, μ_{th}^p ranges for the $K^\pi = 8^-$ states from about $7.3 \, \mu_N$ to about $7.6 \, \mu_N$. This stability results from the fact that, for each set of K^π quantum numbers, the same proton blocked states are involved in all considered nuclei. A stable behavior is also observed in the values calculated for the $K^\pi = 8^-$ two-neutron configuration along the $N = 106$ isotonic chain, again because the same neutron blocked states are involved in the corresponding nuclei.

In contrast, along the Hf isotopic chain, the calculated magnetic dipole moments of the lowest-energy two-neutron $K^\pi = 6^+$ and $K^\pi = 8^-$ states exhibit some jumps which are due to changes in the blocked configurations. A sizable negative value $\mu_{\text{th}}^n \approx -1.3 \mu_N$ is more precisely found for the $K^\pi = 6^+$ two-neutron ($\frac{5}{2}^+[642]$, $\frac{7}{2}^+[633]$) configuration in the $^{168-172}$Hf isotopes, whereas an almost vanishing value of μ_{th}^n is obtained for the $K^\pi = 6^+$ two-neutron ($\frac{5}{2}^-[512]$, $\frac{7}{2}^-[514]$) configuration from ^{174}Hf up to ^{178}Hf, and finally a rather large negative value $\mu_{\text{th}}^n \approx -2 \, \mu_N$ is found for the $K^\pi = 6^+$ two-neutron ($\frac{5}{2}^-[512]$, $\frac{7}{2}^-[503]$) configuration in the $^{182-186}$Hf isotopes. Similarly, μ_{th}^n takes a rather small value (in μ_N units) between about 0.06 and 0.3 for the $K^\pi = 8^-$ two-neutron ($\frac{7}{2}^-[514]$, $\frac{9}{2}^+[624]$) configuration in $^{168-178}$Hf isotopes, whereas it is large and negative, around $-2 \, \mu_N$, for the $K^\pi = 8^-$ two-neutron ($\frac{7}{2}^-[503]$, $\frac{9}{2}^+[624]$) configuration in the $^{182-186}$Hf isotopes.

The almost vanishing values of μ_{th}^n found for the $K^\pi = 6^+$ two-neutron ($\frac{5}{2}^-[512]$, $\frac{7}{2}^-[514]$) configuration in $^{174-178}$Hf can be ascribed to a cancellation mechanism explained in detail in Ref. [41]. On the one hand, the two blocked neutron orbitals have approximately opposite spin projections on the symmetry axis, so that the spin contribution to the intrinsic part μ_{intr} of μ_{th}^n almost vanishes. This opposite spin content in the two-neutron blocked configuration is visible in the dominant Nilsson quantum numbers $\frac{5}{2}^-[512]$ (spin up) and $\frac{7}{2}^-[514]$) (spin down) for the $K^\pi = 6^+$ states for example. Note also that, for neutrons, the orbital-momentum contribution to μ_{intr} is zero. On the other hand, the collective contribution μ_{coll} to μ_{th}^n is positive and of the order of a few tenths of μ_N. One thus concludes that the net spin contribution from the intrinsic part of the magnetic dipole moment is slightly negative and has approximately the same absolute value as μ_{coll}. This cancellation mechanism is less pronounced

in the $K^\pi = 8^-$ two-neutron states of $^{168-178}$Hf and in the considered $N = 106$ isotones (see Table II) with μ_{th}^n between about 0.06 and 0.35 (in μ_N units).

On the other hand, sizable (or even large) negative values of μ_{th}^n testify to a spin-aligned two-neutron blocked configuration, as can readily be seen in the dominant Nilsson quantum numbers in the $(\frac{5}{2}^+[642], \frac{7}{2}^+[633])$ (spins up) configuration for the $K^\pi = 6^+$ isomeric state in the lighter Hf isotopes, in the $(\frac{5}{2}^-[512], \frac{7}{2}^-[503])$ (spins down) configuration for the $K^\pi = 6^+$ state in the heavier Hf isotopes and in $(\frac{7}{2}^-[503], \frac{9}{2}^+[624])$ (spins up) for the $K^\pi = 8^-$ state in the $^{182-186}$Hf isotopes.

Overall we can say that the calculated value for the magnetic dipole moment in a considered two-quasiparticle configuration can strongly constrain the choice of the corresponding neutron or proton blocked states whenever relevant experimental information is available. In this context, the comparison with μ_{exp} of μ_{th}^n and μ_{th}^p can help confirm the configuration of an isomeric state. This is, e.g., the case of the $K^\pi = 6^+$ isomer in ^{172,174,178}Hf isotopes, which all have a measured magnetic moment of about $5.6 \, \mu_N$ that is very well reproduced by the two-proton configuration $(\frac{5}{2}^+[402], \frac{7}{2}^+[404])$. Moreover these isotopes have an excitation energy of about 1.6 MeV, overestimated by about 600 keV in our calculations. Although the lowest-lying two-neutron configurations provide a significantly better agreement with E_{exp}^* in ^{172,174,178}Hf isotopes, they have a magnetic dipole moment, in strong disagreement with the experiment. Therefore the 6^+ isomeric state of ^{172,174,178}Hf isotopes is most likely of pure proton two-quasiparticle character. In the same spirit, the comparison of μ_{th}^n and μ_{th}^p with μ_{exp} for the 8^- isomeric state in ^{176}Yb favors the interpretation of a neutron two-quasiparticle configuration for this state. Indeed, although μ_{th}^n has the wrong sign, it differs much less from μ_{exp} than μ_{th}^p does. Moreover the calculated excitation energy of the neutron configuration agrees very well with experiment.

The case of the $K^\pi = 8^-$ isomeric state in ^{178}Hf is particularly interesting for two reasons. On the one hand, the measured magnetic dipole moment $\mu_{\text{exp}} = 3.09 \, \mu_N$ considerably differs from the one measured in the neighboring even Hf isotopes, namely $\mu_{\text{exp}} = 7.93 \, \mu_N$ in ^{176}Hf and $\mu_{\text{exp}} = 8.7 \, \mu_N$ in ^{180}Hf. On the other hand, μ_{th}^n and μ_{th}^p calculated respectively for the lowest-energy neutron and proton $K^\pi = 8^-$ configurations in ^{178}Hf strongly deviate from the measured magnetic dipole moment. At the same time the calculated excitation energies E_{th}^{*n} and E_{th}^{*p} are both in fair agreement with experiment. Since the experimental value μ_{exp} is kind of *sandwiched* between our theoretical estimates μ_{th}^n and μ_{th}^p, one could guess that the 8^- isomeric state in ^{178}Hf is a mixture of the two-neutron $(7/2^-[514], 9/2^+[624])$ configuration and the two-proton $(7/2^+[404], 9/2^-[514])$ configuration.

We could even attempt to estimate the weight of each configuration by the following simple model. Let us assume that the 8^- isomeric state $|\Psi\rangle$ can be written as a superposition $|\Psi\rangle = \alpha |\Psi_n\rangle + \beta |\Psi_p\rangle$, where $|\Psi_n\rangle$ denotes the SHFBCS solution corresponding to the two-neutron configuration and

$|\Psi_p\rangle$ the one corresponding to the two-proton configuration, both normalized to unity.

The coefficients α and β are assumed to be real and to satisfy $\alpha^2 + \beta^2 = 1$. Since the intrinsic magnetic dipole moment operator $\hat{\mu}_z$ commutes with the third component of the isospin operator and because it is a one-body operator, it cannot couple $|\Psi_n\rangle$ and $|\Psi_p\rangle$, so we have

$$\langle\Psi|\hat{\mu}_z|\Psi\rangle = \alpha^2 \langle\Psi_n|\hat{\mu}_z|\Psi_n\rangle + (1 - \alpha^2) \langle\Psi_p|\hat{\mu}_z|\Psi_p\rangle. \quad (2)$$

One then can estimate the total magnetic dipole moment as

$$\mu_{\text{th}}(\alpha^2) = \alpha^2 \mu_{\text{th}}^n + (1 - \alpha^2)\mu_{\text{th}}^p \quad (3)$$

and, equating it with μ_{exp}, one can deduce α^2 to find

$$\alpha^2 = \frac{\mu_{\text{th}}^p - \mu_{\text{exp}}}{\mu_{\text{th}}^n + \mu_{\text{th}}^p} \approx 0.56 \quad (4)$$

and $\beta^2 = 0.44$. The neutron and proton configurations are therefore estimated to account for respectively 56% and 44% to the 8^- isomeric state corroborating the assessment in Ref. [55] and references quoted therein.

IV. SUMMARY AND CONCLUDING REMARKS

We explored series of $K^\pi = 6^+$ and $K^\pi = 8^-$ isomeric states in the isotopic and isotonic chains of even-even nuclei around ^{178}Hf within the Skyrme (SIII) Hartree-Fock-BCS approach. The calculations made for the corresponding neutron and proton two-quasiparticle configurations outline the systematic behavior of the theoretical 6^+ and 8^- excitation energies in the Hf isotopes and 8^- energies in the $N = 106$ isotones. The comparison with available experimental data provides a test of the SIII Skyrme-Hartree-Fock-BCS approach, as well as of the considered neutron and proton configurations.

We can outline the following findings with the relevant comments:

(i) In the hafnium isotopic chain the overall systematic behavior of the calculated $K^\pi = 6^+$ and $K^\pi = 8^-$ two-quasiparticle excitation energies and magnetic dipole moments compared to the available experimental data for the corresponding K-isomeric states suggests the dominance of the proton over the neutron configurations. At the same time the model suggests the presence of a mixing between the proton and neutron configurations in the 6^+ excitations in ^{174,178}Hf and the 8^- excitations in ^{174,178}Hf. Also, a possible exception with a dominance of the neutron 6^+ configuration in ^{176}Hf could be expected as it appears with the lowest energy while the corresponding magnetic moment is experimentally unknown.

(ii) In the $N = 106$ isotonic chain the overall systematic behavior of the calculated $K^\pi = 8^-$ two-quasiparticle excitation energies suggests the dominance of the neutron over the proton configurations with an exception in ^{178}Hf where possible mixing between the two configurations is identified. The latter is supported by the intermediate value of the corresponding experimental magnetic moment while the former (neutron configuration dominance) is supported by the magnetic moment of the $K^\pi = 8^-$ isomer in ^{176}Yb.

(iii) Regarding the comparison between the theory and experiment, we note that while some discrepancies between the theoretical and experimental energy up to about 300 keV outline the possible limits in the accuracy of the model interpretation (as in, e.g., the 6^+ isomer of ^{176}Hf above), the overall systematic behavior of the $K^\pi = 6^+$ and $K^\pi = 8^-$ isomer energies in the Hf isotopes and $N = 106$ isotones is rather well reproduced. At the same time, complementing the model analysis by good reproduction of available magnetic moments data allows for a rather clear identification of the neutron or proton character of the excitation and thus provides a plausible overall pattern for the evolution of the two-quasiparticle K isomers in the hafnium and translanthanide mass region.

(iv) The comparison to results of RHB calculations with DD-ME2 and DD-PC1 functionals in Ref. [44] shows a similarity in the structure and energy behavior of the corresponding two-quasiparticle configurations, as well as in the quality of the model descriptions for the $K^\pi = 6^+$ and $K^\pi = 8^-$ excitations in hafnium isotopes. More considerable discrepancy between the two approaches is observed for the $K^\pi = 8^-$ excitations in the $N = 106$ isotones, which calls for further detailed comparison. We note that in [44] no theoretical values for the magnetic moments in the considered configurations are given, which would be very useful for the better comparison of the two approaches. Also, we remark that a comparison to the HFB approach with Gogny effective interaction as applied in, e.g., [42] would be very interesting whenever results of corresponding systematic study are available.

(v) The present systematic SHFBCS description of K isomers in the rare-earth and translanthanide nuclei, together with the recent model application to heavy and superheavy nuclei [41], provide a comprehensive test of both the pairing strengths and the SIII Skyrme parametrization used. Therefore, the overall result opens the way to at least two possible developments: (1) readjustment of the pairing strengths taking into account wide range of isomer energies; (2) adding the K-isomer description to a new Skyrme adjustment procedure.

Finally, we conclude that, despite some limited imperfections in the relative energies between the s.p. states, globally our approach to well deformed rare-earth and translanthanide nuclei provides a rather good description of their occurrence around the Fermi energies on two counts: the good reproduction of the general trend of the isomeric energies for the proton configurations under study on one hand, and on the other hand the occurrence of a mixing of neutron and proton configurations at the right place (at least clearly in the 8^- case). Moreover, the good reproduction of magnetic dipole moments indicates that their spin structure is rather well described. This is encouraging for further exploration of other well-documented high-K structures in the same mass region of heavy rare-earth nuclei and nearby.

[1] P. M. Walker and G. D. Dracoulis, Nature (London) **399**, 35 (1999).
[2] R.-D. Herzberg and P. T. Greenlees, Prog. Part. Nucl. Phys. **61**, 674 (2008).
[3] P. Walker and Z. Podolyák, Phys. Scr. **95**, 044004 (2020).
[4] G. D. Dracoulis, P. M. Walker, and F. G. Kondev, Rep. Prog. Phys. **79**, 076301 (2016).
[5] R. Yokoyama *et al.*, Phys. Rev. C **95**, 034313 (2017).
[6] D. J. Hartley, F. G. Kondev *et al.*, Phys. Rev. C **101**, 044301 (2020).
[7] C. M. Petrache *et al.*, Phys. Rev. C **108**, 014317 (2023).
[8] H. M. David *et al.*, Phys. Rev. Lett. **115**, 132502 (2015).
[9] S. S. Hota *et al.*, Phys. Rev. C **94**, 021303(R) (2016).
[10] U. Shirwadkar *et al.*, Phys. Rev. C **100**, 034309 (2019).
[11] J. Kallunkathariyil *et al.*, Phys. Rev. C **101**, 011301(R) (2020).
[12] J. Khuyagbaatar *et al.*, Nucl. Phys. A **994**, 121662 (2020).
[13] J. Khuyagbaatar *et al.*, Phys. Rev. C **103**, 064303 (2021).
[14] K. Kessaci *et al.*, Phys. Rev. C **104**, 044609 (2021).
[15] R. Orlandi *et al.*, Phys. Rev. C **106**, 064301 (2022).
[16] R. Chakma *et al.*, Phys. Rev. C **107**, 014326 (2023).
[17] F. P. Hessberger, arXiv:2309.10468.
[18] F. G. Kondev, M. Wang, W. J. Huang, S. Naimi, and G. Audi, Chin. Phys. C **45**, 030001 (2021).
[19] S. Garg, B. Maheshwari, B. Singh, Y. Sun, A. Goel, and A. K. Jain, At. Data Nucl. Data Tables **150**, 101546 (2023).
[20] P. M. Walker and F. R. Xu, Phys. Scr. **91**, 013010 (2016).
[21] P. Ring and P. Schuck, *The Nuclear Many-Body Problem* (Springer-Verlag, New York, 1980).
[22] H. L. Liu, F. R. Xu, Y. Sun, P. M. Walker, and R. Wyss, Eur. Phys. J. A **47**, 135 (2011).
[23] H. L. Liu and F. R. Xu, Phys. Rev. C **87**, 067304 (2013).
[24] H. L. Liu, P. M. Walker, and F. R. Xu, Phys. Rev. C **89**, 044304 (2014).
[25] X. M. Fu, F. R. Xu, J. C. Pei, C. F. Jiao, Yue Shi, Z. H. Zhang, and Y. A. Lei, Phys. Rev. C **87**, 044319 (2013).
[26] X. M. Fu, F. R. Xu, C. F. Jiao, W. Y. Liang, J. C. Pei, and H. L. Liu, Phys. Rev. C **89**, 054301 (2014).
[27] Y.-C. Yang, Y. Sun, S.-J. Zhu, M. Guidry, and C.-L. Wu, J. Phys. G: Nucl. Part. Phys. **37**, 085110 (2010).
[28] F.-Q. Chen, Y. Sun, P. M. Walker, G. D. Dracoulis, Y. R. Shimizu, and J. A. Sheikh, J. Phys. G: Nucl. Part. Phys. **40**, 015101 (2013).
[29] C. F. Jiao, Yue Shi, H. L. Liu, F. R. Xu, and P. M. Walker, Phys. Rev. C **91**, 034309 (2015).
[30] Z.-H. Zhang, Phys. Rev. C **98**, 034304 (2018).
[31] X.-T. He and Y.-C. Li, Phys. Rev. C **98**, 064314 (2018).
[32] X.-T. He, S.-Y. Zhao, Z.-H. Zhang, and Z.-Z. Ren, Chin. Phys. C **44**, 034106 (2020).
[33] N. Minkov and P. Walker, Phys. Scr. **89**, 054021 (2014).
[34] P. Jachimowicz, M. Kowal, and J. Skalski, Phys. Rev. C **92**, 044306 (2015).
[35] P. Jachimowicz, M. Kowal, and J. Skalski, Phys. Rev. C **98**, 014320 (2018).

[36] P. Jachimowicz, M. Kowal, and J. Skalski, Phys. Rev. C **108**, 064309 (2023).

[37] G. G. Adamian, N. V. Antonenko, and W. Scheid, Phys. Rev. C **81**, 024320 (2010).

[38] T. M. Shneidman, N. Minkov, G. G. Adamian, and N. V. Antonenko, Phys. Rev. C **106**, 014310 (2022).

[39] J. Dobaczewski, A. V. Afanasjev, M. Bender, L. M. Robledo, and Y. Shi, Nucl. Phys. A **944**, 388 (2015).

[40] S. K. Ghorui and C. R. Praharaj, Eur. Phys. J. A **54**, 163 (2018).

[41] N. Minkov, L. Bonneau, P. Quentin, J. Bartel, H. Molique, and D. Ivanova, Phys. Rev. C **105**, 044329 (2022).

[42] L. M. Robledo, J. Phys. G: Nucl. Part. Phys. **51**, 045108 (2024).

[43] V. Prassa, B.-N. Lu, T. Nikšić, D. Ackermann, and D. Vretenar, Phys. Rev. C **91**, 034324 (2015).

[44] K. E. Karakatsanis, G. A. Lalazissis, V. Prassa, and P. Ring, Phys. Rev. C **102**, 034311 (2020).

[45] M. Bender, P. Bonche, T. Duguet, and P.-H. Heenen, Nucl. Phys. A **723**, 354 (2003).

[46] N. Schunck, J. Dobaczewski, J. McDonnell, J. More, W. Nazarewicz, J. Sarich, and M. V. Stoitsov, Phys. Rev. C **81**, 024316 (2010).

[47] Y. Shi, J. Dobaczewski, and P. T. Greenlees, Phys. Rev. C **89**, 034309 (2014).

[48] M. Beiner, H. Flocard, N. Van Giai, and P. Quentin, Nucl. Phys. A **238**, 29 (1975).

[49] L. Bonneau, N. Minkov, D. D. Duc, P. Quentin, and J. Bartel, Phys. Rev. C **91**, 054307 (2015).

[50] J. Damgaard, H. C. Pauli, V. V. Pashkevich, and V. M. Strutinsky, Nucl. Phys. A **135**, 432 (1969).

[51] N. M. Nor, N.-A. Rezle, K.-W. Kelvin Lee, L. Bonneau, and P. Quentin, Phys. Rev. C **99**, 064306 (2019).

[52] L. Bonneau, P. Quentin, N. Minkov, D. Ivanova, J. Bartel, H. Molique, and M.-H. Koh, Bulg. J. Phys. **46**, 366 (2019).

[53] http://www.nndc.bnl.gov/ensdf/.

[54] B. Pritychenko, M. Birch, B. Singh, and M. Horoi, At. Data Nucl. Data Tables **107**, 1 (2016).

[55] T. L. Khoo and G. Løvhøiden, Phys. Lett. B **67**, 271 (1977).

[56] N. J. Stone, IAEA Report No. INDC(NDS)-0794, 2019, https://doi.org/10.61092/iaea.yjpc-cns6.

[57] N. J. Stone, IAEA Report No. INDC(NDS)-0816, 2020, https://doi.org/10.61092/iaea.1p48-p6c6.

[58] P. M. Walker, D. Ward, O. Häusser, H. R. Andreas, and T. Faestermann, Nucl. Phys. A **349**, 1 (1980).

[59] M. L. Bissell *et al.*, Phys. Lett. B **645**, 330 (2007).

[60] H. J. Körner, F. E. Wagner, and B. D. Dunlap, Phys. Rev. Lett. **27**, 1593 (1971).